

# A thermal-driven silicon micro *xy*-stage integrated with piezoresistive sensors for nano-positioning

Young-Soo Choi, Yan Zhang and Dong-Weon Lee<sup>1</sup>

MEMS and Nanotechnology Laboratory, School of Mechanical Systems Engineering,  
Chonnam National University, Gwangju, Korea

E-mail: [mems@jnu.ac.kr](mailto:mems@jnu.ac.kr)

Received 4 July 2011, in final form 10 December 2011

Published 29 March 2012

Online at [stacks.iop.org/JMM/22/055002](http://stacks.iop.org/JMM/22/055002)

## Abstract

This paper describes a novel micro *xy*-stage, driven by double-hot arm horizontal thermal micro-actuators integrated with a piezoresistive sensor (PS) for low-voltage operation and precise control. This micro *xy*-stage structure is linked with chevron beams and optimized to amplify the displacement generated by the micro-actuators that provide a pull force to the movable platform. The PS employed for *in situ* displacement detection and feedback control is fabricated at the base of a cold arm, which minimizes the influence of temperature change induced by electro-thermal heating. The micro *xy*-stage structure is defined through the use of a simple micromachining process, released by backside wet etching with a special tool. For an input power of approximately 44 mW, each chevron actuator provides about 16  $\mu\text{m}$  and the total displacement of the platform is close to 32  $\mu\text{m}$ . The sensitivity of the PS is better than 1 mV  $\mu\text{m}^{-1}$ , obtained from the amplified voltage output of the Wheatstone bridge circuit. The potential applications of the proposed micro *xy*-stage lie in micro- or nano-manipulation, as well as the positioning of ultra-small objects in nanotechnology.

(Some figures may appear in colour only in the online journal)

## Introduction

Micro *xy*-stages have been widely used as popular micro tools in micro- and nano-science and technology since their appearance in the 1990s. Early micro *xy*-stage design is realized by the use of comb-driven micro-actuators with high aspect ratio structures for large forces and displacement [1]. However, the electrostatic actuator requires several tens of volts for reliable operation. Other types of excitation micro-actuators are based on the piezoelectric effect [2], shape memory alloy [3], the electromagnetic method [4] and electro-thermal mechanisms [5, 6]. The fabrication of a piezoelectric actuator requires ultrahigh precision manufacturing with correspondingly high costs [7–10]. Some common actuation mechanisms and their characteristics for microelectromechanical system (MEMS) applications are summarized in table 1. Thermal actuation with low power

consumption has drawn increasing attention due to its large force output within a simple design structure.

The most prominent applications of the micro *xy*-stages include probe-based data storage devices, micro-assembling systems, micro-optical scanners and manipulation of tiny objects such as bio-molecules in microscopes [11–15]. Micro *xy*-stages with different characteristics have been designed for certain specific applications in research activities based on the fundamental principles mentioned above [14, 16–21]. A capability for highly accurate positioning is also very important for *xy*-stage systems used in nanoinstruments, especially for the manipulation of tiny objects. However, little attention is paid to the smallest motion producible by a particular stage in conventional designs, because it is too complex for the design and integration of both sensors and actuators on MEMS devices. Both conventional optical [22] and capacitive detection [23] systems deal with relatively large volumes and scaled down versions are not suited for use as detection mechanisms on a smaller scale. A capacitive sensor

<sup>1</sup> Author to whom any correspondence should be addressed.

**Table 1.** Common actuation mechanisms and their characteristics for MEMS applications

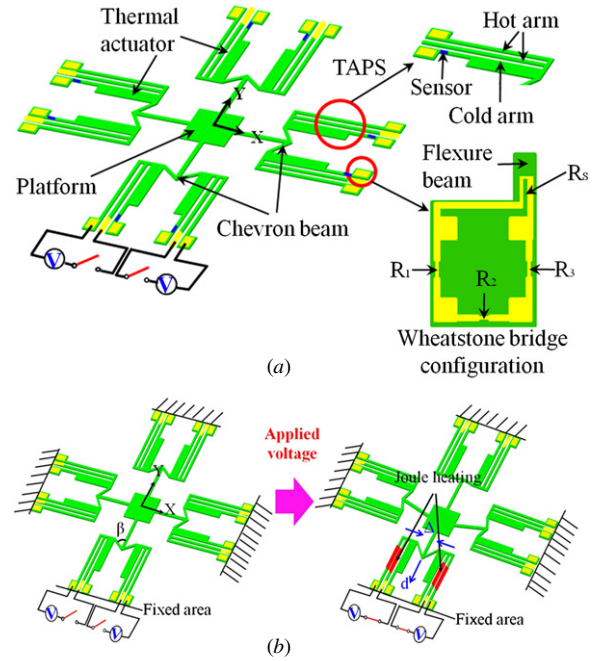
Properties	Electrostatic	Electromagnetic	Piezoelectric	Thermal
Elastic energy density ( $\text{J cm}^{-3}$ )	0.0015	0.025	1	0.4
Specific work ( $\text{J kg}^{-1}$ )	0.08–3	5–50	70–2000	20–700
Displacement	Medium	Large	Medium	Large
Frequency (kHz)	20–80	20–90	30–110	0.06–0.3

may have a parasitic capacitance that could have an effect on the system during displacement measurement. A piezoresistive sensor has a much simpler structure and is thus easy to integrate with other elements through conventional micro-machining processes. Recently, a nano-positioning *xy*-stage with good performance has been presented, consisting of a comb-driven electrostatic micro-actuator and a piezoresistive sensor on the sidewall surface [24]. The drawback of this *xy*-stage is that it results in relatively small levels of displacement. The comb-drive actuators employed to move a central platform also require the use of high voltages, over 28 V, and the displacement approximately  $10\text{ }\mu\text{m}$  is not enough to justify its use in practical applications.

In this paper, a new thermal micro *xy*-stage integrated with a piezoresistive sensor is proposed for *in situ* detection and highly accurate positioning. The prototype of the *xy*-stage is based on a double-hot arm horizontal thermal micro-actuator integrated with piezoresistive sensors, as realized in a previous work [25]. A symmetric array of micro-actuators is optimized for further amplification in displacement. The *xy*-stage is fabricated on one single-crystal silicon layer using conventional MEMS processes. Four piezoresistors positioned on each cold arm of the thermal micro-actuators measure the actuator bending and control power levels for accurate motion of the micro-actuators. The micro-actuator bending has a linear relation with the resultant displacement of the *xy*-stage.

### Design of the micro *xy*-stage

The proposed electro-thermal micro-actuator has a simple structure and can be easily micro machined through conventional MEMS processes. The micro *xy*-stage is capable of generating large displacements and forces with relatively low-power consumption [26]. Thermal actuators are conventionally composed of either V-beam or U-beam structures that resistively heat up when a voltage is applied. The resulting thermal expansion in an axial direction caused by the Joule heating is converted into mechanical motion. To generate sufficient motion in the V-beam actuators, heat needs to be generated through all of the beams. A piezoresistive sensor cannot be integrated on a V-beam surface due to the temperature dependence of the sensor. The principle of the U-beam actuator also relies on passing a current through a U-shaped structure with two arms possessing different geometric properties. A cold arm used in the U-beam actuator has less influence on the temperature change than a comparable arm in a V-beam actuator. However, a small change of temperature on the cold arm can still influence the sensitivity of a piezoresistive sensor. This issue can be solved by adding another hot arm to the current U-beam design. The cold arm

**Figure 1.** (a) Diagram and (b) principle of the proposed micro *xy*-stage.

will thus be free from the current flow and the temperature rise. This additional hot arm can also improve the power efficiency of the thermal micro-actuator, when compared to conventional single-hot arm U-beam actuators [27]. When a current passes through the outer and inner hot arms, both arms are resistively heated to a higher temperature, leading to a thermal expansion that is larger than in the cold arm. The difference in thermal expansion between the cold and hot arms causes the actuator to rotate about the flexure. A micro *xy*-stage with translational motion to the *X*- and *Y*-axes needs a component with the ability to convert rotational motion to translational motion. This is realized by using arrays of two hot-arm horizontal thermal micro-actuators combined with chevron beams. The chevron beams combined with the actuators convert the rotational motion of the thermal actuator to linear translational motion. Displacement of the *xy*-stage is amplified and maximized by optimization of the chevron beams' angles. To prevent the buckling effect that could be expected in four linked beams, a tractive structure attached to the link beam, connected between the chevron beam and the platform, is also optimized. Figure 1(a) shows a schematic diagram of the proposed micro *xy*-stage.

The micro *xy*-stage has an overall size of  $9\text{ mm} \times 9\text{ mm}$  and consists of eight thermal micro-actuators integrated with a piezoresistive sensor (TAPS), four chevron beams, four link beams and one platform in the center. The actuation principle

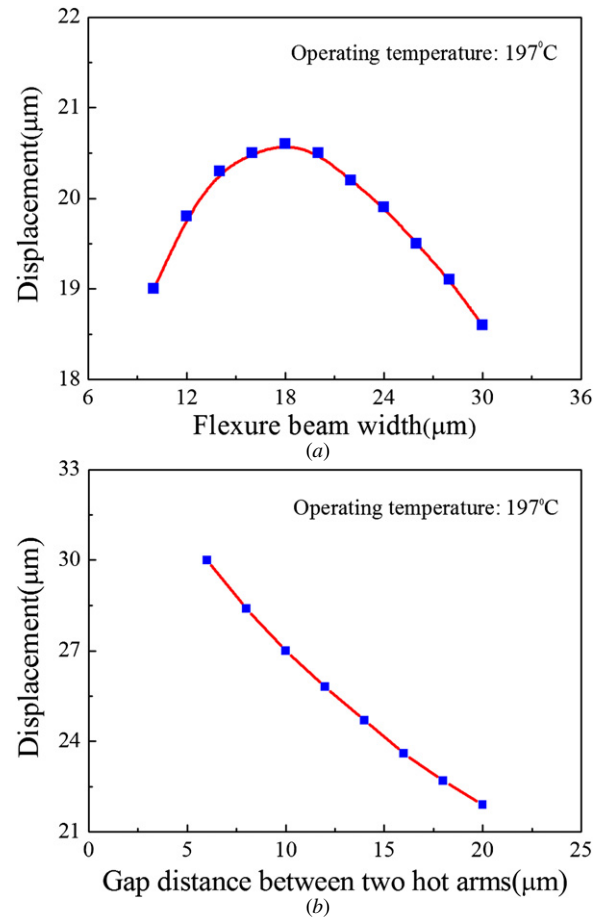
**Table 2.** Material properties of silicon used in the simulation

Parameters (unit)	Value
Modulus of elasticity $E$ (GPa)	162
Density ( $\text{kg m}^{-3}$ )	2330
Poisson ratio $\nu$	0.22
Thermal expansion coefficient ( $\text{ppm K}^{-1}$ )	2568
Thermal conductivity ( $\text{W mK}^{-1}$ )	148

of the proposed micro  $xy$ -stage is shown in figure 1(b). A pair of TAPS are aligned in parallel and connected by a chevron beam at the end of each TAPS, this provides displacement in the  $+X$ - and  $-X$ -directions. The thermally induced deflections,  $\Delta$ , at the end of each TAPS are transformed into a sum of the chevron beam displacements,  $d$ , in the  $+Y$ - or  $-Y$ -direction with amplification  $d = \frac{\Delta}{\cos \beta}$ , where  $\beta$  is one-half of the angle of the chevron beam. The deflection,  $\Delta$ , can be monitored by using the integrated piezoresistor on each TAPS. Four identical pairs of TAPS with chevron beams are arranged perpendicular to one another in order to move the central platform in-plane along the  $+X$ -,  $-X$ -,  $+Y$ - and  $-Y$ -axes. Each pair is connected to the four extended cantilever beams from the center platform. The sensing piezoresistor is integrated with the thermal actuator, and three other resistors are also formed on the  $xy$ -stage body with the same geometry and process conditions. This arrangement forms a Wheatstone bridge for displacement detection and further control of the power applied to the thermal micro-actuator, thereby providing reliable movement.

### Finite element simulation

Finite-element modeling is used for proper optimization of the proposed micro  $xy$ -stage. This software, ANSYS, allows for coupling of a thermal model that describes electrical heating, conduction and convection cooling to a structural model that describes deformation caused by constrained thermal expansion. The change of material properties caused by convection and radiation is assumed to be negligible because both have minimal effects on practical operation of the thermal actuator at lower input power levels. The characteristic parameters used for the simulation are listed in table 2. Analysis of the micro  $xy$ -stage is carried out using SOLID98 10-node tetrahedral coupled field elements with both VOLT and TEMP degrees of freedom. The optimization of the micro  $xy$ -stage is largely divided into two parts: optimization of the single thermal actuator and optimization of the connected chevron beams. To obtain the maximum displacement of the thermal actuator, we study the influence of the flexure beam width, the gap between two hot arms and the angle between thermal actuators and chevron beams. In addition, the width of the cold arm and the flexure is optimized at the operating temperature of 200 °C. From the simulation results, it can be seen that maximum displacement is obtained with flexure beam and cold arm widths of 19  $\mu\text{m}$  and 80  $\mu\text{m}$ , respectively. The narrow width of the flexure beam results in a lower spring constant and a larger stress sensitivity. However, the buckling phenomenon that occurs at the flexure joint and the cold

**Figure 2.** Displacement of the thermal microactuator influenced by (a) flexure width, and (b) gap distance.

arm could reduce platform displacement. Figure 2(a) shows simulation results of the effect that the width of the flexure has on displacement. The gap distance between two hot arms also affects the performance of the thermal actuator, as shown in figure 2(b), where  $t$  is the thickness of the micro  $xy$ -actuator. The displacement of the thermal actuator increases as the gap decreases. In addition, the movement range of the platform could be influenced by the angle between the actuator and the chevron beam.

### Fabrication

Figure 3(a) shows a schematic diagram of the micromachining process for the micro  $xy$ -stage. A 30 mm  $\times$  30 mm silicon-on-insulator (SOI) wafer with corresponding layer thicknesses of 10  $\mu\text{m}$  for the device layer, 1  $\mu\text{m}$  for the buried oxide layer and 325  $\mu\text{m}$  for the handle layer is used as a starting material for the micro-stage fabrication. The electrical resistivity of the device layer measured by a four-point-probe is approximately 3.5  $\Omega \text{ cm}$ . After the standard cleaning process, 500 nm thick  $\text{SiO}_2$  is grown in a wet ambient environment at 1000 °C by using a furnace, which is used as an additional protection layer for backside silicon etching in a tetramethylammonium hydroxide (TMAH) solution. The backside of the wafer, coated with  $\text{SiO}_2$ , is further protected by a layer of photoresist, which

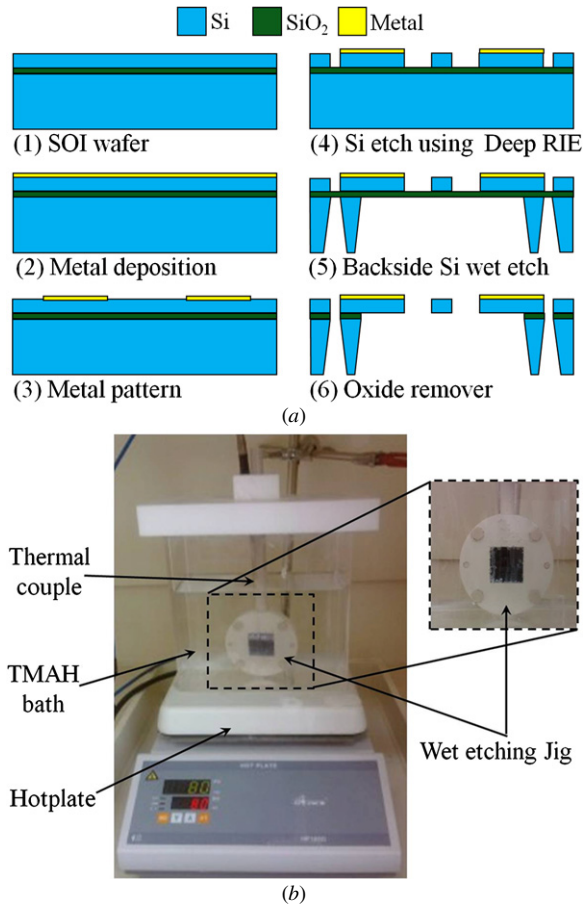


**Figure 3.** (a) Fabrication process of the micro xy-stage, and (b) an optical image of a teflon jig for back side Si etch.

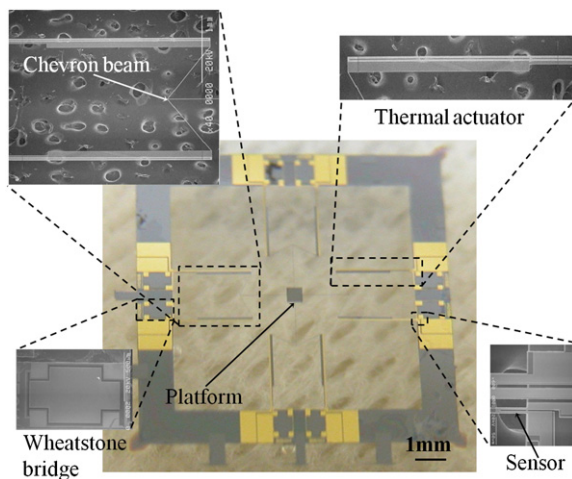


**Figure 4.** Optical images of the fabricated device. Inserts show close-up views of the xy-stage.

is then completely removed. The SiO<sub>2</sub> layer on the front side is removed with a buffered hydrofluoric acid (BHF) solution. A metal layer of Cr/Au (50/80 nm) is deposited by sputtering, and patterned for both the wire leads and piezoresistive sensors through a lift-off process using an AZ 5214 photoresist, which is then removed in an acetone solution. The 10  $\mu$ m thick single-crystal silicon micro xy-stage is defined by deep reactive ion etching, with a 1.4  $\mu$ m thick photoresist mask

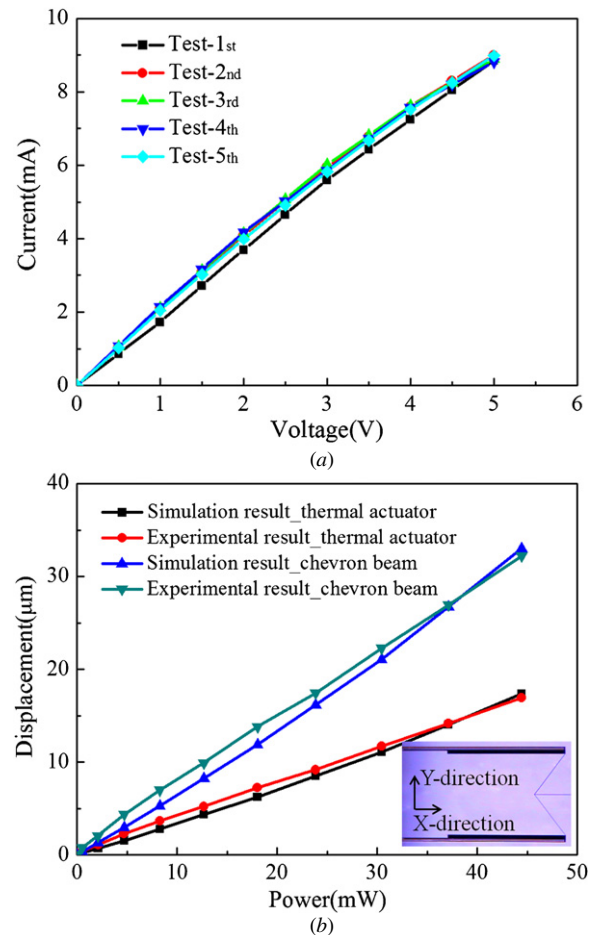


**Figure 5.** (a) *I*-*V* curves of five test samples of the thermal microactuator, and (b) displacement of the thermal microactuators (Y-direction) and the chevron beam (X-direction), respectively.

as the protective layer. The 325  $\mu$ m thick silicon layer on the backside is wet etched using a 20% TMAH solution at 80  $^{\circ}$ C, with the buried oxide of the SOI wafer as an etch-stop layer. During wet etching, the front side of the wafer is protected with a backside wet etching jig, because it is very difficult to protect the front side with typical masking layers, such as metals or photoresists. Pinhole free micro xy-stages are successfully fabricated by the use of the jig designed for wafers of 30 mm  $\times$  30 mm in dimension, as shown in figure 3(b). The possible fabrication thickness using the wet-etching jig depends on the open area of the buried oxide layer exposed to the TMAH solution. In our design, it remains problematic to keep the wet etching until the buried oxide layer is completely exposed to the TMAH solution. The solution pressure results in undesired small cracks in the buried oxide layer when the thickness of the diaphragm is below 15  $\mu$ m. Hence, the TMAH solution may pass through the cracks to the front side of the wafer before the solution completely removes the handling layer to be etched out. This may destroy a certain part of the xy-stage structure formed on the device layer. Another protective layer of SU-8 2050 is spin-coated on the front side of the wafer. This layer not only increases the diaphragm stiffness, but also protects the xy-stage structure from the TMAH solution. The SU-8 is easily removed in a



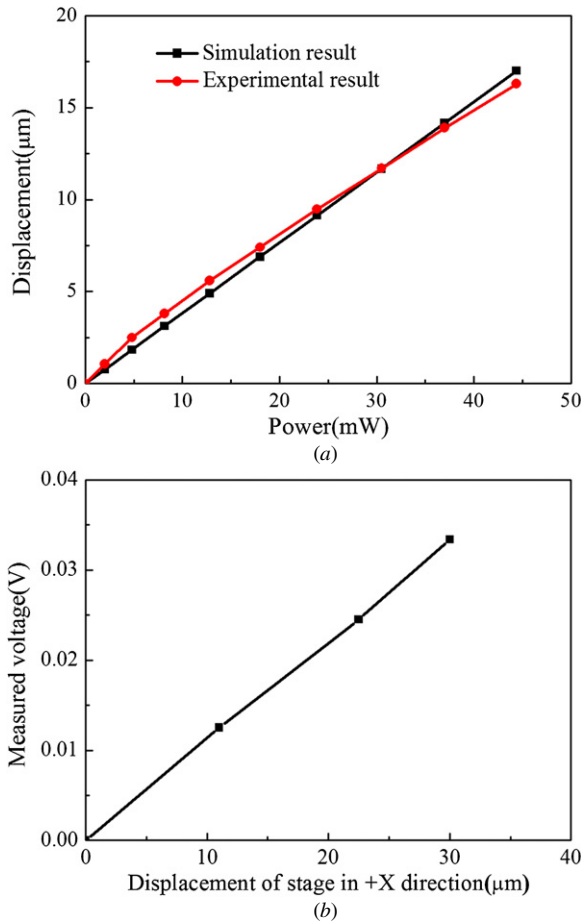


**Figure 6.** The electro-thermally induced displacement of the movable platform as (a) a function of applied power, and (b) the measured output voltage of the Wheatstone bridge with the displacement of the micro xy-stage.

remover PGA, followed by the removal of the buried oxide in BHF (6:1). The fabricated device is cleaned with DI water, rinsed with isopropyl alcohol (IPA) solution and finally dried in air. Optical images of the fabricated xy-stage are shown in figure 4.

## Experimental results

In order to verify the reliable actuation capability of the micro xy-stage, the  $I$ - $V$  curve of the thermal actuator is measured. Five samples are tested in this experiment, as shown in figure 5(a). The electrical resistance of the thermal actuator is measured to be approximately 0.6 k $\Omega$ . The small discrepancy in resistance is due to fabrication imperfections that affect the size of the actuator structure. Both the optical microscope and CCD camera can measure the displacement of the thermal actuators and micro xy-stage. Figure 5(b) shows the measured displacement of the fabricated the thermal actuators ( $Y$ -direction) and the chevron beam ( $X$ -direction) as a function of applied power, which is in good agreement with the simulated results. The displacement of the chevron beam is approximately 33  $\mu\text{m}$  when the input power for the actuator is 42 mW. This is roughly two times larger than the displacement of the thermal actuators. The micro xy-stage with symmetric

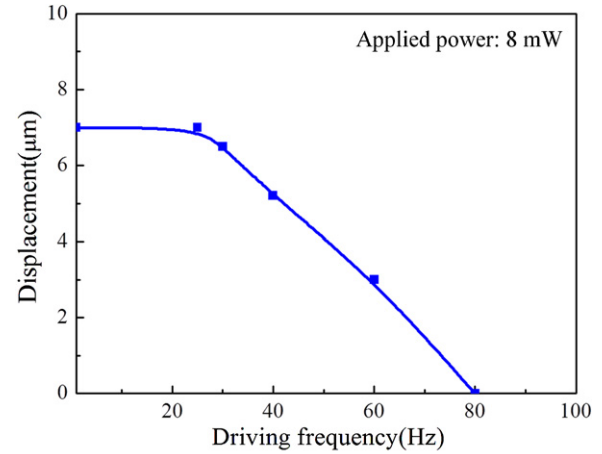


**Figure 7.** Frequency response of the thermal actuator displacement.

configuration is then excited to move in the  $-X$  ( $-Y$ ) and  $+X$  ( $+Y$ ) axial directions. Displacement of 16.1  $\mu\text{m}$  in both  $\pm X$ -directions is obtained with an input power of 44 mW, as shown in figure 6(a). The displacement decrease compared to that of the chevron beam is caused by the platform connected to other actuators. The resultant displacement of the platform is approximately 32.2  $\mu\text{m}$ . The measured displacement of the stage shows a linear relation between movement and applied power.

The micro xy-stage is fabricated via a simple micromachining process and is easily integrated with the reliable piezoresistive sensor, without the use of additional space for *in situ* displacement detection. The sensing piezoresistor, as one of the elements in a Wheatstone bridge, is patterned on the base area of the flexure and the other three are patterned on the substrate, as shown in the schematic diagram in figure 1. The electrical resistance of the piezoresistor is measured as approximately 94  $\Omega$ . For a DC voltage of 4 V applied to the Wheatstone bridge, the output voltage generated by the motion of the stage is amplified with a low noise preamplifier. The measured voltage corresponding to the displacement of the micro xy-stage, plotted in figure 6(b), yields a displacement sensitivity of approximately 1 mV  $\mu\text{m}^{-1}$ . Figure 7 shows the measured frequency response of the thermal actuator displacement of 8 mW actuation power. The resulting actuating speed of 30 ms is quite attractive for the xy-stage application.

## Conclusions

This paper describes a thermal actuator-based micro xy-stage with low power consumption and precise control, fabricated using a simple bulk micromachining process. The proposed micro xy-stage can provide a large displacement of 32.2  $\mu\text{m}$  at 44 mW by using a novel structure. The structure uses a linked chevron beam between two thermal actuators for displacement amplification, which is monitored by an integrated piezoresistive sensor on the thermal actuator, with a sensitivity of 1 mV  $\mu\text{m}^{-1}$ . Of particular note, in order to prevent buckling induced during the movement of the micro xy-stage, we propose a tractive structure of link beams

connected between the chevron beam and the platform. The proposed micro *xy*-stage has potential applications in scanning probe microscopy (SPM)-based high-density storage systems, micro-optical systems and precise manipulation systems.

## Acknowledgments

This work is supported by the National Research Foundation of Korea (NRF) grant funded by the Korea government (MEST) (No. 2007-0056959) and by WCU project (R32-2009-000-20087-0), Republic of Korea.

## References

- [1] Indermuhle P F, Linder C, Brugger J, Jaecklin V P and de Rooij N F 1994 Design and fabrication of an overhanging *xy*-microactuator with integrated tip for scanning surface profiling *Sensors Actuators A* **43** 346
- [2] Yao Q, Ferreira P M and Mukhopadhyay D 2005 Development of a novel piezo-driven parallel-kinematics single crystal silicon micropositioning XY stage *Proc. SPIE Int. Conf. Smart Sensors, Actuators and MEMSII (Seville, Spain, 9–11 May)* **5836** 56
- [3] Li Y, Sasaki M and Hane K 2005 A two-dimensional self-aligning system driven by shape memory alloy actuators *Opt. Laser Technol.* **37** 147
- [4] Choi J J, Park H, Kim K Y and Jeon J U 2001 Electromagnetic micro *x-y* stage with very thick Cu coil for probe-based mass data storage device *Proc. SPIE Int. Conf. Smart Structures and Materials (Newport Beach, USA, 5–7 March)* **4334** 363
- [5] Wu C T and Hsu W 2002 An electro-thermally driven microactuator with two dimensional motion *Microsyst. Technol.* **8** 47
- [6] Luo J K, Flewitt A J, Spearing S M, Fleck N A and Milne W I 2005 Three types of planar structure microspring electro-thermal actuators with insulating beam constraints *J. Micromech. Microeng.* **15** 1527
- [7] Croft D and Devasia S 1999 Vibration compensation for high speed scanning tunneling microscopy *Rev. Sci. Instrum.* **70** 4600
- [8] Lee C W and Kim S W 1997 An ultraprecision stage for alignment of wafers in advanced microlithography *Precis. Eng.* **21** 113
- [9] Ku S S, Pinsopon U, Cetinkunt S and Nakajima S 2000 Design, fabrication, and real-time neutral network control of a three-degrees-of-freedom nanopositioner *IEEE/ASME Trans. Mechatronics* **5** 273
- [10] Ru C H and Sun L N 2005 Improving positioning accuracy of piezoelectric actuators by feedforward hysteresis compensation based on a new mathematical model *Rev. Sci. Instrum.* **76** 095111
- [11] Zhang D Y, Ono T and Esashi M 2005 Piezoactuator-integrated monolithic microstage with six degrees of freedom *Sensors Actuators A* **122** 301
- [12] Toshiyoshi H, Su G J, LaCosse J and Wu M C 2003 A surface micromachined optical scanner array using photoresist lenses fabricated by a thermal reflow process *J. Lightwave Technol.* **21** 1700
- [13] Kwon S H and Lee L P 2002 Stacked two-dimensional micro-lens scanner for micro confocal imaging array *15th IEEE Int. Conf. MEMS (Las Vegas, USA, 20–24 January)* p 483
- [14] Kim C H, Jeong H M, Jeon J U and Kim Y K 2003 Silicon micro XY-stage with a large area shuttle and no-etching holes for SPM-based data storage *J. Microelectromech. Syst.* **12** 470
- [15] Liu X, Kim, K K and Sun Y 2007 A MEMS stage for 3-axis nanopositioning *J. Micromech. Microeng.* **17** 1796
- [16] Tuantranont A, Bright V M, Zhang J, Zhang W, Neff J A and Lee Y C 2001 Optical beam steering using MEMS-controllable microlens array *Sensors Actuators A* **91** 363
- [17] Bernstein J J, Taylor W P, Brazzle J D, Corcoran C J, Kirkos G, Odhner J E, Pareek A, Waelti M and Zai M 2004 Electromagnetically actuated mirror arrays for use in 3-D optical switching applications *J. Microelectromech. Syst.* **13** 526
- [18] Krishnamoorthy U, Lee D S and Solgaard O 2003 Self-aligned vertical electrostatic combdrives for micromirror actuation *J. Microelectromech. Syst.* **12** 458
- [19] Miyajima H, Asaoka N, Isokawa T, Ogata M, Aoki Y, Imai M, Fujimori O, Katashiro M and Matsumoto K 2003 A MEMS electromagnetic optical scanner for a commercial confocal laser scanning microscope *J. Microelectromech. Syst.* **12** 243
- [20] Kim J B and Lin L W 2005 Electrostatic scanning micromirrors using localized plastic deformation of silicon *J. Micromech. Microeng.* **15** 1777
- [21] Zhou L X, Kahn J M and Pister K S J 2006 Scanning micromirrors fabricated by a SOI/SOI wafer-bonding process *J. Microelectromech. Syst.* **15** 24
- [22] Borovic B, Liu A Q, Popa D, Cai H and Lewis F L 2005 Open-loop versus closed-loop control of MEMS devices: choices and issues *J. Micromech. Microeng.* **15** 1917
- [23] Chu L L and Gianchandani Y B 2003 A micromachined 2D positioner with electrothermal actuation and sub-nanometer capacitive sensing *J. Micromech. Microeng.* **13** 279
- [24] Sun L N, Wang J C, Rong W B, Li X X and Bao H F 2008 A silicon integrated micro nano-positioning *xy*-stage for nano-manipulation *J. Micromech. Microeng.* **18** 125004
- [25] Zhang Y, Choi Y S and Lee D W 2010 Monolithic micro-electro-thermal actuator integrated with a lateral displacement sensor *J. Micromech. Microeng.* **20** 085031
- [26] Lee K C and Lee S S 2004 Deep X-ray mask with integrated electro-thermal micro *xy*-stage for 3D fabrication *Sensors Actuators A* **111** 37
- [27] Kolesar E S *et al* 2002 Single- and double-hot arm asymmetrical polysilicon surface micromachined electrothermal microactuators applied to realize a microengine *Thin Solid Film* **420–421** 530